

EFFECT OF POST AND SOIL STRENGTH ON THE PERFORMANCE OF THE MODIFIED ECCENTRIC LOADER BREAKAWAY CABLE TERMINAL (MELT)

GREG S. PATZNER¹
CHUCK A. PLAXICO²
MALCOLM H. RAY³

ABSTRACT

The effect of wood post strength and soil strength on the dynamic performance of guardrail systems has long been a concern of the roadside safety community. Evidence from full-scale crash tests has suggested that these parameters may significantly affect guardrail system performance. Essentially identical tests have resulted in widely varying outcomes that might be the result of varying post strengths and soil conditions.

A finite element model of a common guardrail terminal, the Modified Eccentric Loader Breakaway Cable Terminal (MELT), was developed to examine the effect of post strength and soil strength on the overall performance of the terminal system. A matrix of twelve simulations of a particular full-scale crash test scenario was conducted using the explicit nonlinear dynamic finite element software, LS-DYNA3D to establish the combinations of post and soil strengths that produce favorable results. The parametric simulations show that certain combinations of soil and post strengths increase the hazardous possibilities of wheel snagging, pocketing, or rail penetration, while other combinations produce more favorable results. This parametric study helps identify conditions that will maximize the safety and reliability of the guardrail terminal system.

INTRODUCTION

Guardrail terminals have been a focus of attention in roadside safety research for several decades. Guardrail terminals are one of the most challenging types of roadside hardware to design. Recently, three nearly identical full-scale crash tests of a common guardrail terminal shown in Figure 1, the Modified Eccentric Loader Breakaway Cable Terminal (MELT), produced widely varying results.(1)(2) One possible explanation for the differences was variation in the post strengths and soil conditions. As a result, finite element simulation of this test scenario was conducted to aid in determining the effect of post and soil strength on the performance of the system.

The impact conditions for these full-scale tests consisted of a 2000-kg pickup truck striking the terminal at a 20 degree

1 Applications Engineer, IBM Aerospace Competency Center, 1200 5th Avenue, Seattle WA, 98101.
206-587-2770. gpatzner@us.ibm.com

2 Associate Research Engineer, Civil Engineering, Worcester Polytechnic Institute, Worcester, MA 01609.
508-831-5598. cplaxico@wpi.edu.

3. Associate Professor of Civil Engineering, . Worcester Polytechnic Institute, Worcester, MA 01609.
508-831-5340. mhray@wpi.edu.

angle with a velocity of 100 km/h, corresponding to NCHRP Report 350, test designation 3-35.(3) The impact point was at the third post from the beginning of the installation. The test and simulation configuration is shown in Figure 2. The purpose of this test was to ensure that the terminal was sufficiently anchored to allow the vehicle to redirect. In the first of the three tests (i.e. test MLT-3), Grade No. 2 posts were installed in a moderately strong soil with a typical moisture content of 6.5%. This test resulted in rupture of the guardrail at the splice located at the downstream end of the terminal, and allowed the vehicle to penetrate the barrier. In the second test (i.e. test MLT-4), higher strength Grade No. 1 Dense wood posts were used in the installation. The results of this crash test, however, proved to be unacceptable due to snagging of the front impact side wheel assembly on a guardrail post and the subsequent rollover of the test vehicle. The cause of the wheel snag could not be precisely determined, but relatively wet soil conditions (e.g., moisture content of 10.3%) on the day of the test were suspected to have played a role in the failure. A third test (i.e. test MLT-5) was conducted using Grade No. 1 Dense wood posts mounted in a moderately strong, dry soil. This successful test met all crash testing specifications given in NCHRP Report 350.

SOIL MODELING

A finite element model of the MELT used in the full-scale tests was developed in which the soil and wood post strengths could be varied parametrically.(4)(5) The soil model used the subgrade modulus approach typical of laterally loaded pile analysis, in which the posts are supported by an array of uncoupled nonlinear springs, as shown in Figure 3 (all springs are not shown for simplicity). The horizontal subgrade modulus of the soil, which is used in defining the stiffness of the nonlinear springs, is fundamental in determining the soil resistance against the posts. The subgrade modulus is influenced by many factors such as the relative density, moisture content and cohesiveness of the soil, as well as the overburden pressure, the nature of the applied load, and the material properties and geometry of the post.

The value of the subgrade modulus is usually obtained by means of various empirical relationships that have been presented in the literature. The horizontal subgrade modulus, k_h , is given by the basic relationship:

$$k_h = \frac{F}{A * y} \quad (1)$$

where F is the horizontal reaction force, A is the area over which the force is applied and y is the resulting displacement. The relationships used in the MELT soil model were the ones proposed by Habibagahi and Langer and are based upon the bearing capacity concept where, for a granular non-cohesive soil, the soil reaction force is a function of the overburden stress, σ_e .(6)

$$k_h = N_q \frac{\sigma_e}{y} \quad (2)$$

N_q is a lateral bearing capacity factor which is dependant upon deflection, depth, post width, and the internal angle of friction of the soil. More details on determining the bearing capacity factor can be found in Plaxico et al. (1998).(5) The effective overburden stress, σ_e , can be further modified to incorporate the effect of the moisture content of the soil. The effective overburden stress is given by:

$$\sigma_e = \gamma_e Z \quad (3)$$

where γ_e is the effective unit weight of the soil and Z is the depth below grade. The effective unit weight of the soil can be approximated by the total unit weight of the soil until a certain degree of saturation is reached. The total unit weight of the soil is expressed as::

$$\gamma = \gamma_d(1 + \omega) \quad (4)$$

where ω is the moisture content of the soil. At saturation, the effective unit weight of the soil is reduced due to the pore water pressure that creates separation and floatation of the soil particles. At this point the effective unit weight of the soil is reduced by the unit weight of water and can be represented by:

$$\gamma_{e,sat} = \gamma_{sat} - \gamma_w \quad (5)$$

where γ_{sat} is the total unit weight of the soil at saturation and γ_w is the unit weight of water. As mentioned earlier, adding moisture to the soil slightly increases its strength until a moisture content close to saturation is reached. In static post testing conducted at the Texas Transportation Institute, it was observed that the load carrying capacity of the soil began to decrease sharply at a moisture content that was approximately 75 percent of the moisture content at saturation.(7)

Given the relationship in Equation 5, the decrease in load capacity of the soil due to moisture content nearing saturation levels was incorporated into the effective unit weight of the soil as a decrease proportional to the unit weight of water. A bilinear relationship between the effective unit weight of the soil and the moisture content was created with Equation 4 governing the relationship below 75 percent degree of saturation and the following expression governing the relationship when the moisture content is in excess of 75 percent of saturation:

$$\gamma_e = \gamma_d(1 + \omega) - \left(\frac{\omega - \omega_{75}}{\omega_{sat} - \omega_{75}} \right) \gamma_w \quad (6)$$

Using this relationship, the strength of the soil at its maximum ($\omega = \omega_{75}$) is 108 percent of its strength in perfectly dry conditions ($\omega = 0$), and the strength of the soil in saturated conditions ($\omega = \omega_{sat}$) is 58 percent of the maximum strength of soil with a dry density of $2 \times 10^{-5} \text{ N/mm}^3$ and a moisture content at saturation of 0.11.

WOOD POST MODELING

Modeling the material and physical behavior of timber guardrail posts has been a principal concern to researchers developing finite element models of guardrail systems. While metal materials are relatively easy to characterize and model using standard material models in LS-DYNA3D, timber materials are more challenging. LS-DYNA3D does not contain a material model that is directly applicable to modeling the behavior of wood. Wood is a very complex anisotropic material that is often assumed to be orthotropic. The most formidable method of modeling wood posts is using a material which specifies a criterion for element failure. In this approach, the analyst need not know *a priori* where the failure is going to occur. Unfortunately, most of the LS-DYNA3D material models possessing a failure criterion are isotropic and better suited to metals than wood. Until a material model is developed that encompasses the

complexity of an orthotropic material with failure, however, a simplified isotropic material modeling technique must be used.

The failure mode observed in timber posts is such that the longitudinal fibers of the post progressively fail in tension on the impact face of the post due to bending. The isotropic-elastic-plastic with failure material model (material type 13) in LS-DYNA3D includes failure criteria that enables an element to fail in tension while still supporting compressive loads.⁽⁸⁾ Timber post failure in tension can be adequately simulated with the use of material type 13 in LS-DYNA3D by setting the failure pressure to a value that typifies wooden post failure.

The failure mode of the breakaway timber posts necessitated the use of fourteen-point integration elements in the failure region of the post. A one-point integration rule (default in ls-dyna) would not suffice for this failure condition since a single brick element in bending cannot develop failure stresses. An element using the one-point integration rule only calculates stresses at one point in the center of the volume, which would coincide with the neutral axis of the element in bending. With stresses only being calculated near the neutral axis of the element, failure stresses will not be reached. In early component simulation of the timber posts, the last row of elements on the failure plane of the posts would not fail for this reason.

The eight-point integration scheme was also applied in the failure region of the posts in order to reduce computation time, however, the failure response of the eight-point integrated elements was very inconsistent with the failure criteria (i.e. the failure strain should increase proportionally with failure pressure, but rather varied randomly). This inconsistency is possibly due to excessive hourglassing of the eight-point integrated elements. The fourteen-point integrated elements have no zero energy modes and function as a fully-integrated element. The one-point integrated elements, therefore, were only used in the lower stress regions of the post model and the fourteen-point integrated elements were used in the failure region.

Although many of the basic material parameters for wood, such as the modulus of elasticity, can be found in literature,

typical values of the failure criteria used in material type 13 are not provided in literature. In order to arrive at values of these parameters, an alternative method was necessary. Fortunately, there were numerous ballistic pendulum tests of Grade No. 2 BCT timber posts conducted at the Federal Outdoor Impact Laboratory that could be used for determining parameters that would adequately simulate the failure of a breakaway wood post.⁽⁹⁾ The failure pressure of material type 13 was adjusted in simulations of the pendulum tests such that the acceleration history of the simulation closely corresponded to that of the physical test.⁽⁵⁾ The thirty percent increase in failure pressure from Grade No. 2 posts to Grade No. 1 Dense posts was based on values in literature for the modulus of rupture.

PARAMETRIC STUDY OF THE POST AND SOIL STRENGTH

Twelve finite element simulations were conducted involving three different post strengths and four different soil strengths. The soil strengths were determined by selecting different levels of moisture content, while holding all other parameters constant. The four soil moisture contents corresponded to 50, 75, 87.5, and 100 percent saturation. The three post strengths corresponded to Grade No. 2 and Grade No. 1 Dense posts and a relatively low post strength (about 30% weaker than typical Grade No. 2).

Basically, two potentially hazardous results of a full-scale crash test, pocketing and wheel snagging, were considered in evaluating the matrix of simulations in accordance to NCHRP Report 350. Pocketing is the crash test event in which the impacting vehicle causes large deflections of the guardrail such that a “pocket” is formed in the guardrail and the vehicle can no longer be redirected. Pocketing usually results in penetration or rupture of the guardrail or loss of anchorage of the system. Guardrail rupture typically happens at points of stress concentration such as guardrail splice joints. Wheel snagging is the event in which the wheel assembly of the impacting vehicle directly impacts a post in the system causing extensive damage to the wheel assembly which could result in overturning of the vehicle upon redirection.

The potential for pocketing of the vehicle was determined from measurements of the maximum guardrail deflection during impact as well as the cross section forces observed near the splice that ruptured in the full-scale test. Figure 4

shows the maximum guardrail deflection in each of the simulations. For a given post strength, the maximum guardrail deflection was relatively high for soils with a lower effective unit weight. As the effective unit weight of the soil initially increased, the maximum deflection decreased. This indicates that the soil strength is the parameter governing the dynamic response of guardrail systems installed in soils with a low unit weight. At some critical soil strength, however, the post failure becomes the dominant factor in simulations involving Grade No. 2 and weak Grade No. 2 posts. When the soil becomes strong enough, it induces quicker failure of the posts because stresses are concentrated near the ground line. The result is larger guardrail deflections and increased chances of pocketing.

In simulations involving Grade No. 1 Dense posts, though, the post failure effect never becomes dominant. It appears that at this high post strength, the soil strength remains the dominant factor controlling the amount of guardrail deflection. Maximum guardrail deflection steadily decreased as the effective unit weight of the soil increased (e.g., as the soil becomes more and more stiff) in the Grade No. 1 Dense post simulations. The soil was not able to become strong enough to induce any additional post failure. Any increase in post strength above Grade No. 1 Dense will not greatly affect the performance of the guardrail system.

Regardless of post strength, the amount of soil resistance on the anchor post seemed to create a minor decrease in deflection in soils with a high effective unit weight. As the soil strength was increased beyond the value that induced the maximum number of broken posts, less movement of the end post was observed and, therefore, less guardrail deflection. It was also determined from the simulations that for any given soil strength, as the post strength increases, guardrail deflection decreases. The study demonstrates that weak posts combined with either weak or strong soil produce the greatest potential for pocketing since these conditions produced the largest deflections in the guardrail.

The potential for pocketing, especially causing guardrail rupture, was evaluated from the cross section forces observed near the splice that ruptured in the full-scale test and is shown in Figure 5. In general, the study showed that as the post strength increased, the possibility of guardrail rupture decreased. Also, as the soil strength increased, so did the chances of guardrail rupture. Simulations involving Grade No. 1 Dense posts, however, deviated slightly from the general trends. When Grade No. 1 Dense posts were mounted in a weak soil, the cross section forces were higher than those

observed with weaker posts, but were still well below the magnitude of forces observed in strong soils. The combination of strong soil and weak posts, therefore, was the least favorable condition regarding the potential for guardrail rupture.

The potential for wheel snagging was measured from the peak accelerations of the front impact side wheel assembly. Upon vehicle impact with the fourth post, basically two events can happen. If the fourth post is broken, larger guardrail deflections are created upstream of the fifth post, allowing the traveled path of the vehicle wheel to penetrate deeper into the system. This creates a more direct impact with the fifth post and causes higher accelerations of the wheel assembly. If the fourth post is not broken, then the necessary redirection is provided to reduce the severity of the impact with the fifth post. In this case, the severity of impact is highest at the fourth post.

In the simulations involving Grade No. 1 Dense and Grade No. 2 posts, the fourth post was not broken and the greatest accelerations were experienced when impacting the fourth post. As shown in Figure 6, the peak accelerations observed for the standard Grade No. 2 posts were fairly constant across soil strengths and exhibited relatively lower potential for wheel snagging. Grade No. 1 Dense posts produced slightly higher accelerations in higher strength soils.

The fourth post was broken in each of the simulations containing the weakest posts and created more severe impacts with the fifth post. Accelerations were low for the weak posts in strong soil, but the weak posts produced high accelerations in weaker soils due to the direct impact with the fifth post. The soil was not strong enough to induce quick failure of the fifth post and resulted in elevated accelerations. It could be concluded from the simulation data that strong posts mounted in stronger soils produce the highest magnitude of wheel accelerations, which would imply that these conditions produce the most potential for wheel snag. This is somewhat misleading since the maximum acceleration of the wheel assembly is not the only factor involved in determining vehicle stability due to wheel snag.

Maximum force of the wheel assembly is an important factor, however, the kinematics of the vehicle at the time of wheel snag as well as the number of posts that were hit should also be considered. Although the simulations involving the stronger soils resulted in higher accelerations on the wheel assembly they only involve the wheel contacting one or two posts during impact. So it is reasonable that the greatest potential for vehicle instability due to wheel snag will occur

when either very weak posts (e.g. weaker than Grade No. 2) are mounted in weak soil or when very strong posts (e.g. Grade No. 1 dense) are mounted in weak soil.

This is also evidenced in the full-scale tests. In test MLT-3 Grade No. 2 posts were installed in a very stiff soil. The posts used in this test had been used in an earlier full-scale test and it was believed that some of the posts may have been damaged. This test resulted in several posts breaking and guardrail rupture. Test MLT-4, in which Grade No. 1 Dense posts were mounted in very wet soil conditions, resulted in wheel snag which caused the vehicle to roll over. In test MLT-5 the Grade No.1 Dense posts were mounted in very stiff soil at near optimum moisture conditions and the test was successful.

CONCLUSIONS

During this investigation of the effect of post and soil strength on the performance of the MELT, several hypotheses were conceived in correspondence to each of the measurements for potential failure of the system. Each hypothesis eliminated a portion of the possible post strength and soil strength parameters from those that are likely to produce successful redirection of the vehicle in an NCHRP Report 350 test designation 3-35 impact scenario. Table 1 is a summary of the simulation and test results from the parametric study. Figure 7 shows the three potential failure regions on a plot of the maximum guardrail deflection against the soil effective unit weight and forms a feasible region of post and soil strengths. Although the boundaries created in the study are not firmly set due to the small number of data points, they provide a basic understanding of the effect that the soil strength and post strength have on performance of the MELT in a redirection impact.

ACKNOWLEDGMENTS

The authors would like to thank Mr. Martin Hargrave and Mr. Charlie McDevitt of the Federal Highway Administration's Design Concepts Research Division for supporting this work and providing the crash test data.

REFERENCES

1. Strybos, J., and J. Mayer. “*Full-Scale Crash Evaluation of a Modified Eccentric Loader Terminal*”, NCHRP Report 350 Test Designation 3-35, SwRI Test No. MLT-3. Federal Highway Administration, Washington D.C., February 1997.
2. Patzner, G.S. “*Effect of Wood Post Strength and Soil Strength on the Performance of the Modified Eccentric Loader Breakaway Cable Terminal (MELT) Under Impact Conditions Prescribed by NCHRP Report 350, Test 3-35.*” Masters thesis, University of Iowa, December 1997.
3. Ross Jr., H.E., and D.L. Sicking, R.A. Zimmer, and J.D. Michie. “*Recommended Procedures for the Safety Performance Evaluation of Highway Features.*” National Cooperative Highway Research Program Report 350, Transportation Research Board, Washington D.C., March 1993.
4. Ray, M.H., and G.S. Patzner. “*A Finite Element Model of the Modified Eccentric Loader Breakaway Cable Terminal (MELT).*” Transportation Research Board, 1997.
5. Plaxico, C.A., and G.S. Patzner and M.H. Ray. “*Finite Element Modeling of Guardrail Timber Posts and the Post-Soil Interaction*” Transportation Research Board, 1998.
6. K. Habibagahi and J.A. Langer. “*Horizontal Subgrade Modulus of Granular Soils*”, Laterally Loaded Deep Foundations. ASTM Special Technical Publication 835, Langer, Mosely, and Thompson, editors. American Society for Testing Materials 1984, pp. 21-34.
7. H.E. Ross Jr. and T.J. Dolf. “*Pull-out Capacity of a Yielding Signpost as Related to Soil Moisture.*” Texas Transportation Institute, Texas A&M University, College Station, Texas, August 1979.
8. J.O. Hallquist, D.W. Stillman and T.L. Lin, *LS-DYNA3D Users Manual-Version 930*, “*A Nonlinear, Explicit, Three-Dimensional Finite Element Code for Solid and Structural Mechanics.*” Livermore Software Technology Corporation, April 1994.
9. C.M. Brown. “*Pendulum Testing of BCT Wood Posts, FOIL Tests: 91P039 through 91P045.*” Federal Outdoor Impact Laboratory, McLean, Virginia, August 1991.

Table 1: Summary of simulation and test results from the parametric study

Soil Effective Unit Weight	CRT Post Type		
	Grade No. 1 Dense	Grade No. 2	Weak Post
12510 N/mm ³	Wheel Snag [Test MLT-4]	Pass	Pocket
17150 N/mm ³	Wheel Snag	Pass	Pass
21200 N/mm ³	Pass	Pass	Rupture
21760 N/mm ³	Pass [Test MLT-5]	Possible Rupture	Rupture [Test MLT-3]



Figure 1. Modified Eccentric Loader Breakaway Cable Terminal

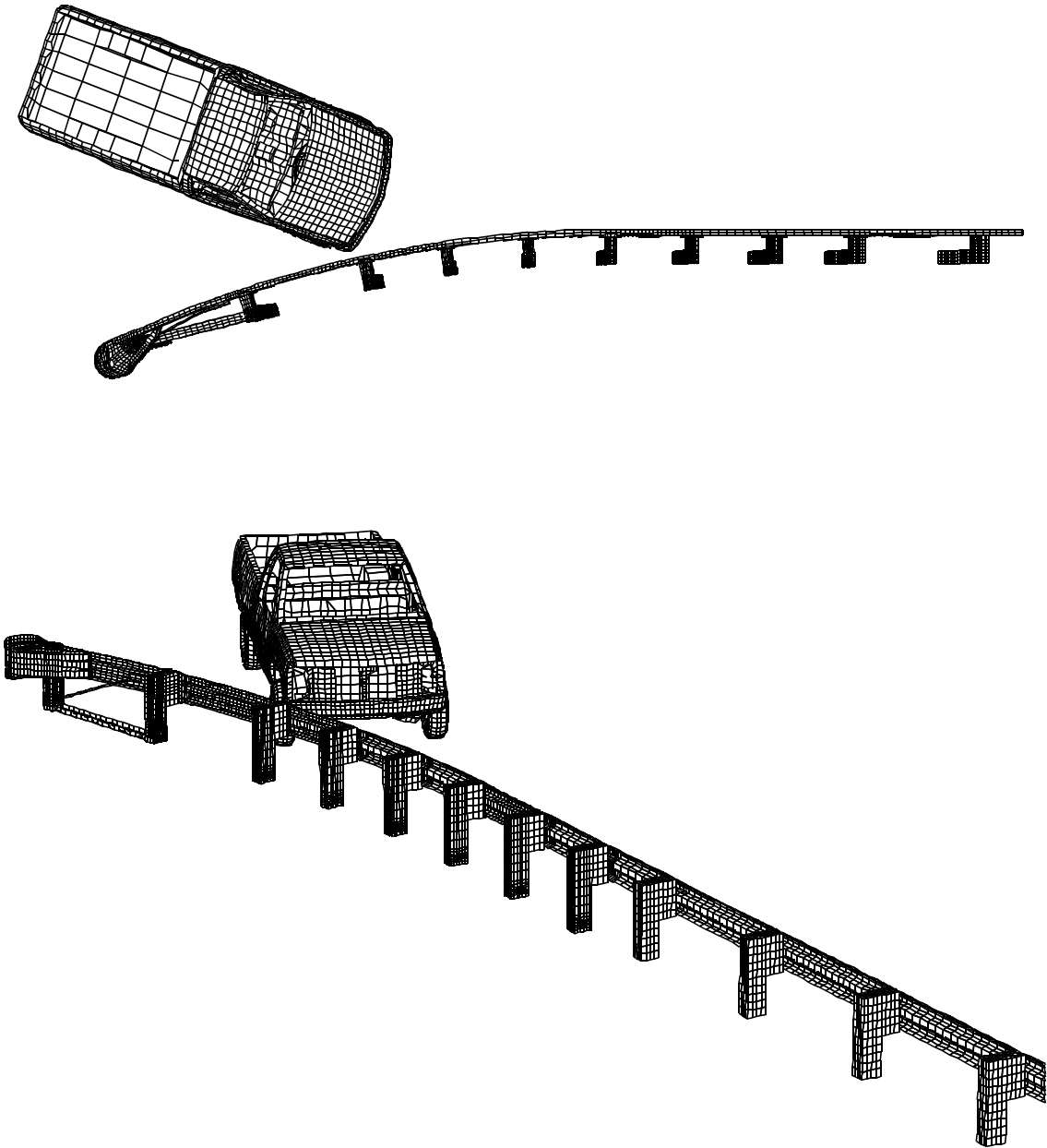


Figure 2. Test and Simulation Configuration

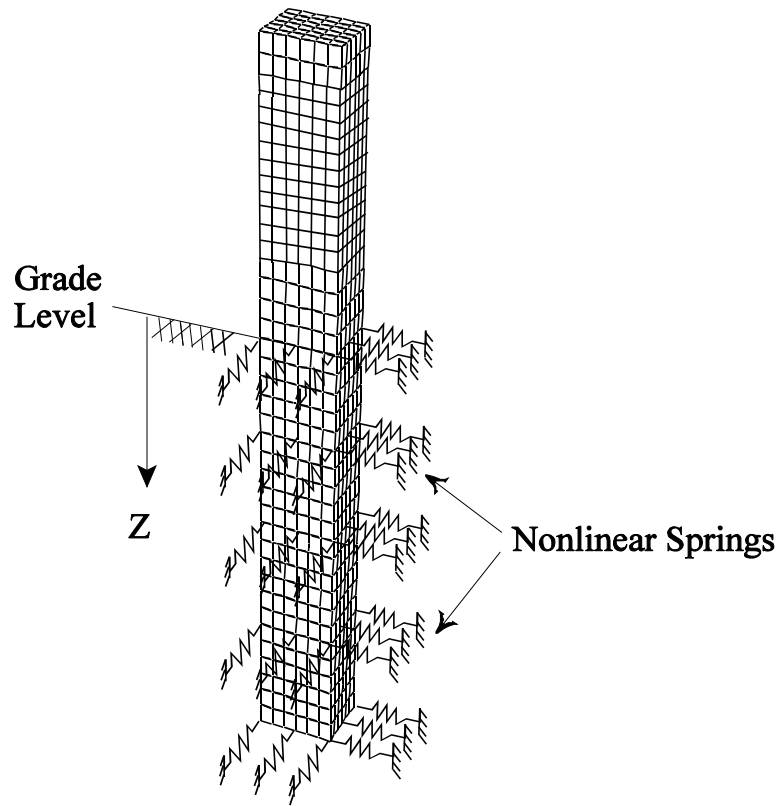


Figure 3. Soil resistance modeled using nonlinear springs

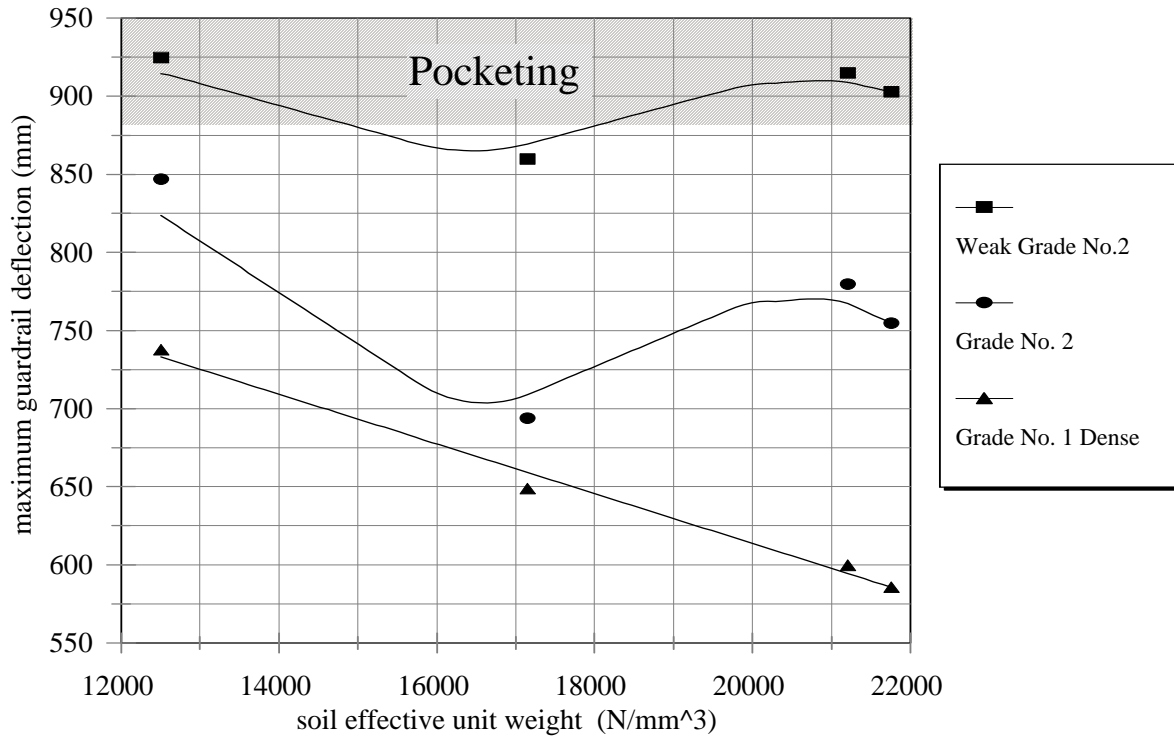


Figure 4. Effect of post and soil strength on the potential for pocketing (guardrail deflection)

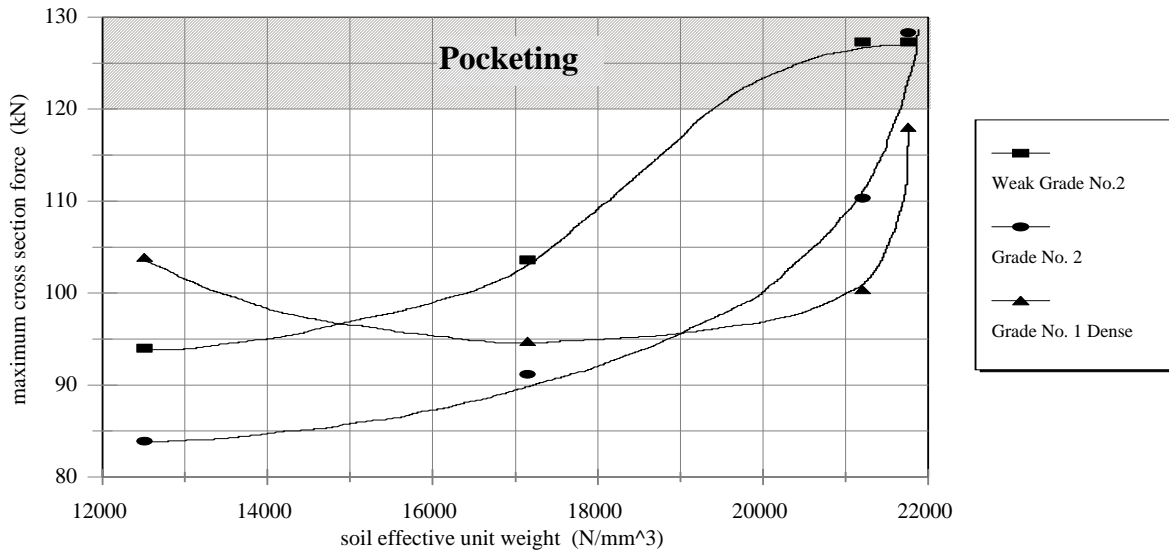


Figure 5. Effect of post and soil strength on the potential for pocketing (cross section forces)

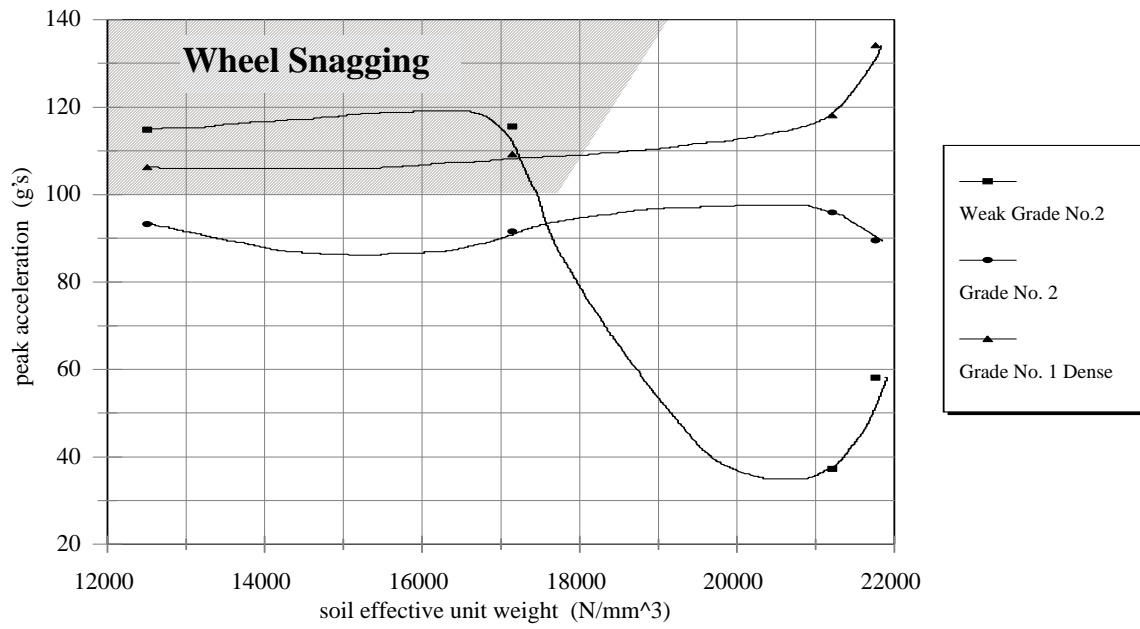


Figure 6. Effect of post and soil strength on the potential for wheel snagging

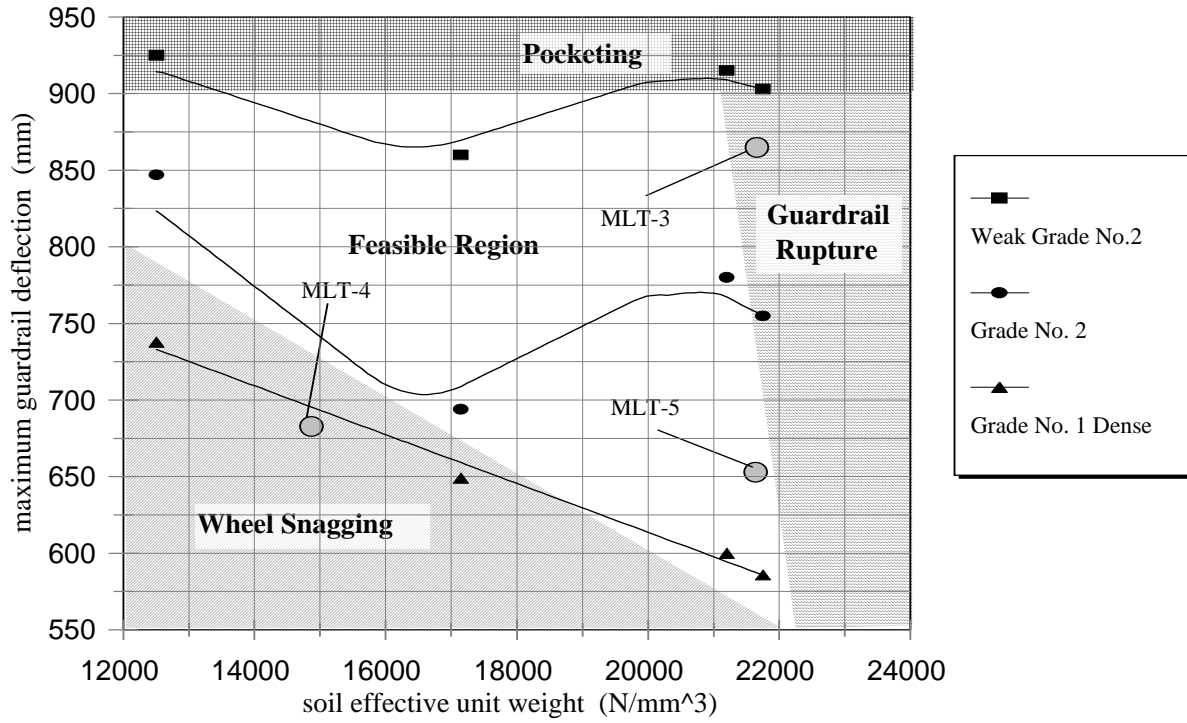


Figure 7. Feasible region of post and soil strengths